RADIO SCIENCE, VOL. 37, NO. 1, 1009, 10.1029/2000RS002602, 2002

Characterization of Leonid meteor head echo data collected using the VHF-UHF Advanced Research Projects Agency Long-Range Tracking and Instrumentation Radar (ALTAIR)

S. Close, S. M. Hunt, and F. M. McKeen

MIT Lincoln Laboratory, Lexington, Massachusetts, USA

M. J. Minardi

Department of Electrical Engineering, Wright State University, Dayton, Ohio, USA

Received 28 December 2000; revised 2 July 2001; accepted 20 September 2001; published 16 February 2002.

[1] The Leonid meteor shower, which was predicted to hit storm-like activity on 17 November 1998, was observed using radar and optical sensors at the Kwajalein Missile Range in order to study potential threats to orbiting spacecraft. Meteor head echo data were collected during the predicted peak of the "storm" primarily using the Advanced Research Projects Agency Long-Range Tracking and Instrumentation Radar (ALTAIR). ALTAIR is a dual-frequency radar at VHF (160 MHz) and UHF (422 MHz) that is uniquely suited for detecting meteor head echoes due to high sensitivity, precise calibration, and the ability to record radar data at a high rate (Gb/min). ALTAIR transmits right-circular (RC) polarized energy and records left-circular (LC) sum, RC sum, LC azimuth angle difference, and LC elevation angle difference channels; these four measurements facilitate the determination of three-dimensional target position and velocity as a function of radar cross section and time. During the predicted peak of the storm, ALTAIR detected 734 VHF head echoes in 29 min of data and 472 UHF head echoes in 17 min of data, as well as numerous specular and nonspecular ionization trails. This paper contains analysis on the head echo data, including dual-frequency statistics and the variability of head echo decelerations. We also include results from the analysis of the radius-density parameter, which shows a strong correlation with deceleration. *INDEX TERMS:* 6245 Planetology: Solar System Objects: Meteors; 6952 Radio Science: Radar atmospheric physics; *KEYWORDS:* meteors, meteoroids, radar, ionosphere, Leonids

1. Introduction

[2] Meteoroids that enter the Earth's atmosphere collide with the neutral air molecules and generate localized ionization regions. These plasma regions are formed primarily within the *E* region of the ionosphere (approximately 80- to 140-km altitude) and are grouped into two categories, including the ionization trail and a locally ionized region that surrounds the meteoroid. Echoes from this locally ionized region are called head echoes when they are detected by radar. A head echo will travel at the same velocity as the meteoroids itself [*McKinley*, 1955], with a radar scattering crosssection (RCS) that is dependent upon the size, shape, composition, and velocity of the meteor. The instantaneous size of a meteoroid is dependent upon the rate of mass dissipation, which, in turn, is dependent upon air density and meteoroid velocity. Radar cross sections will vary between particles and change rapidly as a meteoroid travels through the ionosphere [*Mathews et al.*, 1997]. From the analysis of head echoes, one can deduce meteoroids decelerations and densities, which are independent of ionization assumptions in the formulation applied here.

[3] A renewed interest in meteors resulted from the expected increase in the Leonid meteor flux, due to the recent passage of the comet Tempel-Tuttle (the shower's origin). The last Leonid meteor storm occurred 33 years ago in 1966, commensurate with Temple-Tuttle's 33-year orbital period, and at that time there were few satellites in orbit. Because of the large increase in the satellite population, which currently exceeds 700 operational spacecraft, a worldwide meteor data collection effort was initiated in 1998 to help characterize the Leonid

Copyright 2002 by the American Geophysical Union.
0048-6604/02/2000RS002602$11.00

storm and its potential threat. Kwajlein Missile Range (KMR) was first requested to support the worldwide effort by the Air Force Office of Scientific Research (P. Worden, U.S. Space Command at Peterson Air Force Base in Colorado, private communication, 1998; P. Brown University of Western Ontario, private communication, 1998), and data were collected on the Perseids and Leonids in 1998, as well as the Leonids in 1999. Most of these data were obtained using Advanced Research Projects Agency (ARPA) Long-Range Tracking and Instrumentation Radar (ALTAIR).

[4] ALTAIR resides in the central Pacific at 9°N and 167°E on the island of Roi-Namur in the Kwajalein Atoll, Republic of the Marshall Islands. ALTAIR is a high-power, dual-frequency radar that is capable of collecting precise measurements on small targets at long ranges. ALTAIR utilizes a 46-m diameter, mechanically steered, parabolic dish and transmits a peak power of 6 MW simultaneously at two frequencies, including 160 MHz (VHF) and 422 MHz (UHF). The 46-m-diameter antenna employs a focal point VHF feed and multimode Cassegrain UHF feed in conjunction with a frequency selective sub-reflector (5.5 m diameter). Targets are illuminated with right-circularly (RC) polarized energy in a narrow half-power beam width of 2.8° and 1.1° at VHF and UHF, respectively. A RC polarization signal is transmitted, and the dual-polarization feed horns enable separate reception of left-circular (LC) and right-circular polarization; these measurements are denoted sum left circular and sum right circular. ALTAIR's receive horns are also used to collect LC signal returns for the purpose of angle measurement. The receivers are offset from the focus of the dish, and their signal energies are differenced to produce two additional channels of data, including the left circular azimuth difference (ALC) and left-circular elevation difference (ELC). ALC and ELC are combined in a process known as amplitude comparison monopulse [*Skolnik*, 1990], a form of phase interferometry, to measure the angle of arrival of the radar return (for each pulse) to a small fraction of the beam width. The average angular measurement accuracy, or standard deviation, of the ALTAIR system is 11.2 mdeg in azimuth and elevation at UHF; this value will be higher for returns off of a plasma. The angular accuracy is derived from orbit solutions computed using Earth-orbiting calibration spheres that are routinely tracked by ALTAIR and the NASA laser-ranging network. The results from the numerical orbit fit process are also used to assess ALTAIR's residual range errors. Using the most accurate ALTAIR waveforms, the range accuracy is, on average, 5.0 m. ALTAIR's UHF and VHF RCS is also regularly calibrated using a known target, typically a 56-cm balloon-borne sphere; the absolute RCS measurement capability of ALTAIR is within 0.5 dB.

[5] ALTAIR is part of the Kwajalein Missile Range (KMR), whose mission areas include support of missile testing (such as operational tests of fielded ballistic missile systems) and developmental testing of missile defense systems. ALTAIR itself has a second and much larger mission area, which is to provide support to U.S. Space Command for space surveillance. ALTAIR dedicates 128 hours per week to Space Command and provides data on nearly every space surveillance event involving Earth-orbiting satellites. ALTAIR's high peak power and large aperture combine to create high system sensitivity. Using the most sensitive waveforms available, ALTAIR can reliably detect a target as small as −74 decibels-relative-to-a-square-meter (dBsm) at VHF (−80 dBsm at UHF) at a range of 100km; −80 dBsm is equivalent to 10^{-8} m^2. This high system sensitivity makes ALTAIR very well suited for the detection of small head echoes, which travel with the meteoroid's velocity. These velocity measurements are subsequently used to determine meteoroid decelerations, sizes, and densities that are input into models that determine the impact on orbiting satellites.

2. Leonid Observations

[6] Leonid data were collected on 18 November 1998, during a 3-hour period, which was designed to span the predicted peak of the Leonid storm (0730 local time); Table 1 contains a summary of KMR observation times (12 hours ahead of UT) and the estimated flux rates for the total number of detections and those that occurred primarily within the main beam. These rates were computed by counting the total number of head echoes that were detected during an observation period (typically, 2 min) and then dividing by the time. Over 26 Gb of ALTAIR data corresponding to 30 min of actual measurements were collected during this period, including both on-radiant and off-radiant observations. While the radar is pointing at the radiant, Leonid particles follow paths roughly aligned with the antenna beam and will therefore endure longer in the beam. The purpose of the off-radiant data was to try and observe more of the sporadic meteors and possibly have a greater chance of observing specular meteor trails. For this activity, ALTAIR operated simultaneously at VHF (160 MHz) and UHF (422 MHz). Amplitude and phase data were

Table 1. Summary of Activity During the Leonid 1998 Storm

Time	Elevation	Position	Total Flux, s^{-1}	Main Beam Flux, s^{-1}
1500 GMT[a]	29°	radiant	0.32	0.18
1515 GMT[a]	31°	off-radiant	0.18	0.08
1820 GMT[b]	72°	radiant	0.44	0.29
2020 GMT[b]	68°	off-radiant	0.50	0.39
2042 GMT[b]	64°	radiant	0.73	0.32
2100 GMT[b]	60°	radiant	1.07	0.73
2120 GMT[b]	55°	off-radiant	0.38	0.28
2130 GMT[b]	53°	radiant	0.23	0.12

[a] Minimum detectable RCS, −74 dBsm at VHF and −80 dBsm at UHF.
[b] Minimum detectable RCS, −55 dBsm at VHF and −75 dBsm at UHF.

recorded for each frequency and four receive channels: sum right circular, sum left circular, azimuth difference left circular, and elevation difference left circular. Measurements were collected for radar slant ranges corresponding to altitudes spanning 70 to 140 km at VHF and 90 to 110 km at UHF using two different waveforms (one waveform per frequency). The two waveforms used to collect most of the data were a 40-μs VHF pulse (30-m range sample spacing) and a 150-μs UHF pulse (7.5-m range sample spacing). We used a 333-Hz pulse repetition frequency to provide a high sampling rate in order to better study a meteor's deceleration. Different waveforms (V260M/U1000) were also applied for their high sensitivity to obtain the best estimate of the meteoroid flux. The parameters associated with these waveforms are contained in Table 2.

[7] ALTAIR has a number of sibling radars located at KMR, including Tracking and Discrimination Experiment (TRADEX), which operates at 1320 and 2951 MHz, and ARPA Lincoln C-band Observables Radar (ALCOR), which operates at 5664 MHz. They are parabolic dish radar systems that have narrower beams and somewhat less sensitivity than ALTAIR has. Simultaneous per pulse data were collected at UHF, VHF, L-band, S-band, C-band, and optical wavelengths during the Leonid 1998 shower and are currently being analyzed.

Table 2. Summary of Waveform Parameters for the Leonid 1998 Storm

	V40H	U150	V260M	U1000
Frequency, MHz	160	422	158	422
Bandwidth, MHz	3	18	1	1
PRF, Hz	333	333	50	50
Sample spacing, m	30	7.5	75	75
Sensitivity, dBsm	−55	−75	−74	−80

3. Leonid Data Analysis

[8] Figure 1 is an example of an ALTAIR range-time-intensity (RTI) image. The image shading corresponds to the measured signal-to-noise ratio (SNR) for 2 s of LC channel data that contain three meteor head echoes. To obtain these data, the radar amplitude and phase measurements were reduced using signal-processing algorithms developed at MIT Lincoln Laboratory. The first step in the process involves the calculation of the system noise floor and receiver bias estimates. The noise floor for each receiver channel was estimated by averaging the amplitude $\left(\sqrt{I^2 + Q^2}\right)$ for a noise sample region for each data collection interval. System thermal noise and background sky noise are included in the estimates. The receiver biases were estimated by determining the offset of the system noise floor from zero-mean for each receiver value (LC, RC, AZ, and EL). A 10-dB SNR threshold (above the noise floor) is applied to the LC and RC amplitude, and the data from all four

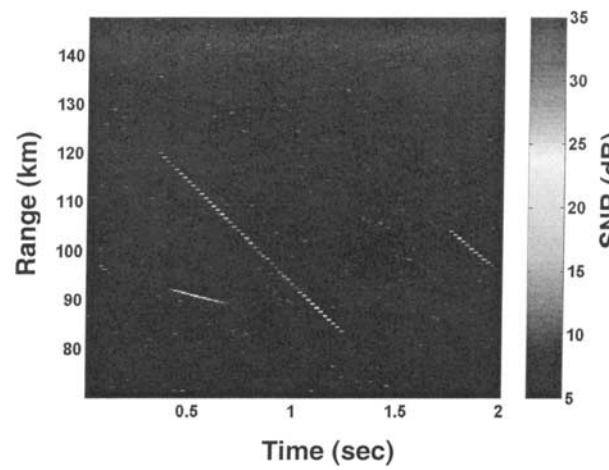

Figure 1. Example range-time-intensity (RTI) image showing three meteor head echoes.

channels are saved whenever either of the thresholds is exceeded.

[9] Digital samples of the received radar pulses are then interpolated to determine the range to the peak amplitude of the LC measurement. The RC, ALC, and ELC receiver measurements are subsequently interpolated to the range of the interpolated LC peak to provide a consistent measurement for all four channels for a given pulse.

[10] Next, a variation of the Hough transform is applied to automatically search the range-time images to associate a series of pulse detections (in straight lines) as one head echo [*Illingworth and Kittler*, 1988]. Suppose we have detected a point (pulse) along a candidate line feature (head echo pulse sequence) at a particular (x, y) coordinate in the range-time image. We know the position of the point, but we do not know the orientation of the candidate line associated with it (e.g., the range-time or velocity direction of the head echo path). Many different lines can pass through a given point, and the point is evidence for any of them, so we test for pulse sequences (lines) with orientations that represent velocities of meteors bound in solar orbit spanning 0 to -72 km/s. A threshold on the length of a pulse detection sequence was used to discard detections not associated with meteors. (The pulse length threshold is a function of radar pulse repetition frequency (PRF) and was set to 5 for a PRF of 333 Hz). The final step in the data reduction process was to use the computed range rates to correct the target ranges for range-Doppler coupling. Range-Doppler coupling is a property of a chirp-type pulse. Doppler shifts of the radar echo cause an offset in the apparent range of the echo. The relationship between target range rate and the range-Doppler coupling range offset [*Fitzgerald*, 1974] is $\Delta r = (Tf_0\nu_r)/B$, where Δr is the range offset, T is the pulse width, f_0 is the radar RF frequency, ν_r is the target radial velocity, and B is the chirp bandwidth. The quantity $(Tf_0)/B$ has units of time and is called the range-Doppler coupling constant. The range-Doppler coupling constants for the ALTAIR waveforms that were primarily used in this study are 2.13×10^{-3} s (VHF) and 3.52×10^{-3} s (UHF).

[11] To obtain meteor decelerations, we extracted each head echo and fit a polynomial curve to its associated time-of-flight velocity profile and interpolated to obtain finer resolution. The data from the two angle difference channels were then processed to determine the angular offset of the detections from the radar boresite (in units of radians). After we applied the angular offsets the three-dimensional (3-D) position of the head echo within the beam was determined. The time rate of change of the 3-D position was computed to obtain the 3-D velocity; a second differentiation resulted in an estimate of the meteor's deceleration. ALTAIR is mainly used as a coherent radar (although sensitive enough to be used as an incoherent radar as well), and Doppler processing of the head echo data to directly measure closing velocity was considered. However, the pulse-to-pulse Doppler processing was not pursued because the PRF and the ALTAIR wavelength of approximately 2 m (VHF) and 0.7m (UHF) give an unambiguous velocity interval of 0.31 km/s and 0.12 km/s, respectively. This was considered too small of an interval for targets with range velocities of the order of 72 km/s.

[12] Monopulse angle measurements are only valid when detections are made in the main beam; therefore care was taken to ensure that the detections that were used did not occur in angle sidelobes. The gain of the two-way ALTAIR antenna falls by more than 30 dB outside the main beam. When the meteor head passes from the main beam into the first sidelobe, the apparent RCS would decrease, and the arithmetic sign of the angle error of one or both of the channels would suddenly change (as if the detection "hopped" to the other side of the beam).

[13] The final goal was to estimate the radius and density of the meteor particle. This was first accomplished by *Evans* [1966] and was explained in reference to ALTAIR data by *Close et al.* [2000]. The final result is

$$r\delta = \frac{3}{2}\nu_m \rho \sec\chi \left(\frac{d\nu_m}{dh}\right)^{-1}, \qquad (1)$$

where r and δ are the radius and density of the meteoroid, respectively, ν_m is the velocity of the meteoroid (or head echo), ρ is the air density (as a function of altitude), h is the height of the head echo, and χ is the elevation (as a function of altitude).

4. Leonid Data Results

4.1. Statistics

[14] Meteor observations were conducted using the ALTAIR system during the Perseid 1998, Leonid 1998, and Leonid 1999 showers. The lowest flux was seen during the Leonid 1999 shower and reached a peak detection rate of approximately one head echo every 10 s; this relatively low value can be explained by the

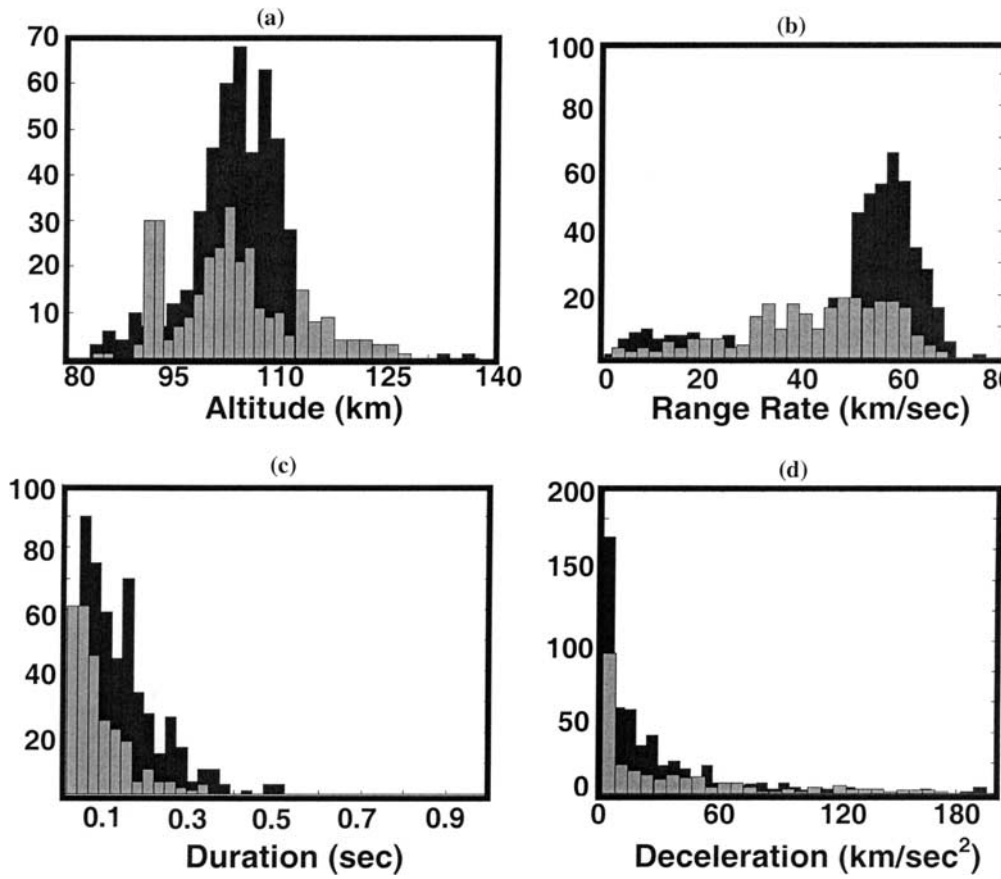

Figure 2. Leonid radiant histograms for 551 VHF head echoes (solid) and 328 UHF head echoes (shaded), including (a) mean detection altitude, (b) range rate, (c) duration, and (d) deceleration.

time of the observations (local noon) and the location of the peak of the storm (Europe) relative to ALTAIR (Pacific Ocean). In contrast, the peak detection rates seen during the Perseid and Leonid 1998 campaigns were one head echo every s and 2 s, respectively. The Leonid 1998 shower also shows a flux variation that reaches a peak near 2100 GMT; these data are contained in Table 1. There is a distinction between the radiant and off-radiant data, as well as a marked increased in the number of particles detected when the storm reached its peak (2100 UT). Our results are slightly inconsistent with observations at Arecibo and European Incoherent Scatter (EISCAT), which showed no significant increase in the detection rate during the shower peak. *Janches et al.* [2000] reported that 1997 Leonid shower observations using Arecibo did not appear to have a detectable effect on the echo rate. *Pellinen-Wannberg et al.* [1998] also did not find a significant increase in meteor rates during showers by using the EISCAT radar. ALTAIR observstions indicate a detectable rise in the background rate during the peak of the Leonid 1998 shower. Orbit determination is currently being pursued; however, at this time we attribute our increased flux to the increased intensity of the Leonid 1998 shower (relative to 1997 and earlier) and also to the fact that we were in prime viewing location. The peak of the storm occurred over the western part of the Pacific Ocean-eastern Asia (ALTAIR's location) when the radiant was almost near zenith.

[15] Figure 2 contains histograms for head echo data collected when ALTAIR was pointed at the Leonid radiant. The plotted results include 551 VHF echoes and 328 UHF echoes that were detected in the ALTAIR main beam; these head echoes had azimuth and elevation data that were within an off-axis angular position of $\pm 1.4^\circ$ and a $\pm 0.6^\circ$ at VHF and UHF, respectively. The total detected rate was 734 VHF echoes in 29 min of data and 472 UHF head echoes in 17 min of data. This detection rate was affected by the presence of intense specular and nonspecular ionization trails that dominated our return signal strength and masked the presence of

head echoes. Also, we believe that only 10–20% of the total number of these head echoes were actually Leonids. We applied the monopulse data to all head echoes and grouped them according to their 3-D velocity and trajectory in order to order to arrive at this percentage. Head echoes that had maximum 3-D velocities less than 65 km/s were categorized as sporadics. The time period with the highest percentage of high-velocity (both range rate and 3-D velocity) head echoes was 2100 UT which is also when the peak flux occurred. The off-radiant data contained the most head echoes with low range rates; the 3-D velocities of the off-radiant head echoes were comparable to on-radiant head echoes.

[16] Figure 1a is a histogram of the maximum detection altitude of both the VHF (solid) and UHF head echoes (shaded). There were 13 VHF head echoes that were detected at an altitude greater than 120 km, and 2 VHF head echoes that were detected at an altitude greater than 130 km. These altitude data are highly correlated with velocity: The highest velocity objects form head echoes at higher altitudes. However, no other noteworthy features (i.e., larger or smaller than typical RCS, duration, or deceleration values) were correlated with these high-altitude head echoes. The two head echoes that formed at altitudes greater than 130 km were both detected at 2100 UT. The head echoes with altitudes between 120 and 130 km were spread among all files, with 2042 and 2130 UT containing the most (four each). None of these high-altitude head echoes have associated nonspecular trails.

[17] Figure 2b contains the histogram for the VHF and UHF mean range rate (slope of the head echo in altitude versus time). The range rate has a smaller error associated with the calculation, relative to the 3-D velocity. Range rate is the radar's line of sight based on the time delay measurements, whereas the 3-D velocity incorporates monopulse angle measurements, which typically can have high errors for reflections from a high-velocity plasma. The range rate distribution indicates several peaks near 71 km/s, 60 km/s, and 30 km/s for both the VHF and UHF data. The 71 km/s peak is believed to be associated with Leonids. The slower peaks are attributed to sporadics; however, the typical velocity of a sporadic is believed to be 20 km/s. The larger "sporadic" velocities seen by ALTAIR most likely correspond to the preferential selection of faster meteors; meteors that have high velocities will have higher RCS values and will therefore be more easily detected by the system. Slow (20 km/s) meteors will have smaller RCS values that can fall below the limiting capability of the radar. Finally, note that several head echoes in Figure 2b were detected with velocities greater than 72 km/s, suggesting an interstellar origin. These interstellar data are currently being examined further.

[18] Figure 2c contains a histogram of the duration times for both the VHF and UHF head echoes and indicates that a typical head echo persists for approximately 0.1 s in the ALTAIR VHF beam (2.8°). The longest head echo endured for nearly 2.3 s in the VHF beam and, in contrast, only 0.4 s in the UHF (1.1°) beam. Longer durations are also correlated with higher RCS and higher velocities.

[19] Figure 2d contains the average decelerations for each of the VHF and UHF head echoes and spanned 4 to 200 km/s^2. The deceleration also showed significant variation over the course of a head echo's life; this will be expanded upon in section 4.2. The change in the head echo's deceleration is correlated with the meteoroid's mass. The largest decelerations were detected for head echoes between 100 and 110 km altitude and also for head echoes that had higher than average RCS values. The correlation between deceleration, altitude, and RCS is discussed by S. Close et al. (Scattering characteristics of high-resolution meteor head echoes detected at multiple frequencies, submitted to *Journal of Geophysical Research*, 2001).

[20] Figure 3 contains the VHF and UHF RCS histograms for both the LC (Figure 3a) and the RC (Figure 3b) RCS data. Both graphs indicate that the average difference between the VHF and UHF data is approximately 24 dBsm; in comparison, trails typically exhibit a much stronger (>35 dBsm) frequency dependence. The UHF cross sections ranged from approximately 3.2×10^{-8} m^2 (limit of the UHF waveform) to 1.0×10^{-2} m^2. The VHF cross sections were between approximately 3.2×10^{-6} m^2 (limit of the VHF waveform) and 1.6×10^{-1} m^2; these values are consistent with *Mathews et al.* [1997] and *Zhou et al.* [1998]. We can explore the wavelength dependence further by comparing the LC and RC RCS values on a per-pulse basis. This technique was applied to 34 head echoes that were detected simultaneously at VHF and UHF. The maximum VHF cross sections were between 12 and 32 dBsm higher than their corresponding maximum UHF detection. By assuming that the RCS is proportional to λ^x, the x values varied from 2.8 to 7.6 and averaged at 4.1.

4.2. Decelerations

[21] Figure 4 contains the first measured results that show that deceleration is not constant over the lifetime of a head echo [*Zhou et al.*, 1998]. Our intuition points to this result as a more realistic characterization of the

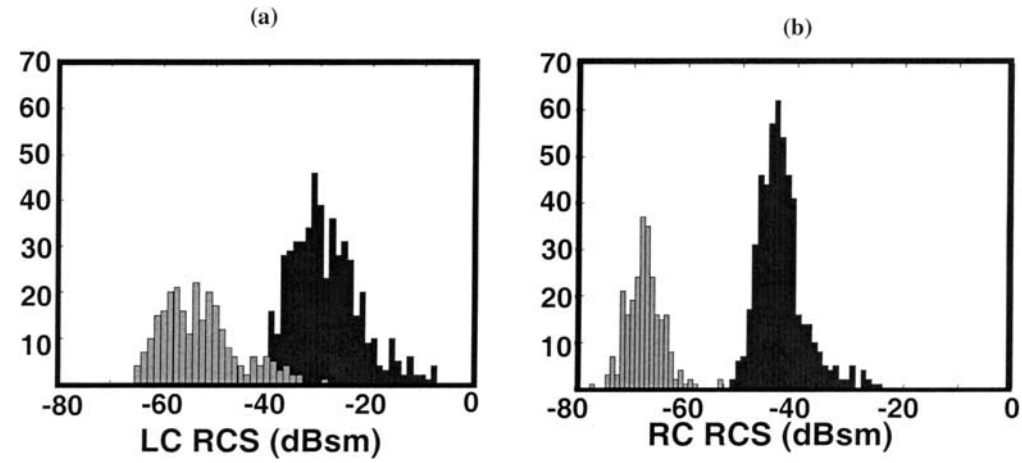

Figure 3. Leonid radiant histograms for 551 VHF head echoes (solid) and 328 UHF head echoes (shaded), including (a) left-circular RCS and (b) right-circular RCS.

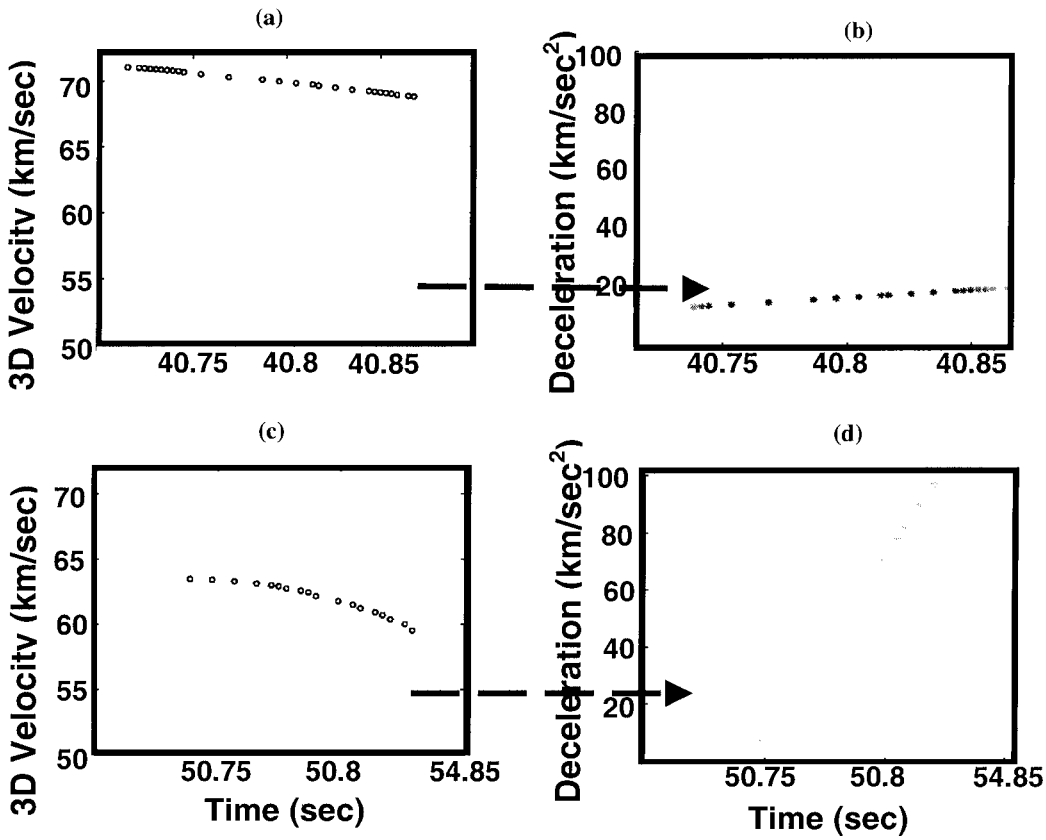

Figure 4. An example head echo showing its (a) true velocity as a function of time and (b) associated deceleration as a function of time. A second example head echo's (c) true velocity and (d) associated deceleration.

Table 3. Summary of Parameters Averaged Over 20 Head Echoes

Parameter	Value
Duration	0.1 s
Maximum RCS	−27 dBsm
Mean apparent velocity	−69 km/s
Deceleration	15 km/s^2
Mean meteor radius-density product	0.08 g/cm^2
Mean radius[a]	0.08 cm
Mean mass	10^{-3} – 10^{-4} g

[a] Assume that meteor density is 1 g/cm^3.

dynamics of a meteor as it traverses the atmosphere. The time-varying deceleration is presumably due to the exponentially increasing atmospheric density and decreasing velocity, coupled with the shape and composition of the meteor itself. Figure 4a shows the 3-D velocity of an example VHF-detected head echo that persisted for over 0.15 s in the beam. Figure 4b is the deceleration (difference with respect to 3-D velocity) and shows that the deceleration varies between 12 and 20 km/s^2. These data were also color-coded (color version not shown here) to show the variation in the LC RCS of the head echo as it decelerates. As a meteor traverses the ALTAIR beam, the returned signal energy will tend to track the spatial distribution of the intensity of the beam pattern. Near the center of the main radar beam, the signal power arriving at the target as a function of angular distance from the center approximately follows a $[\sin(x)/x]^2$ pattern. To characterize this radar artifact, we examined the LC RCS variation of the head echo relative to the beam center. For this particular case the peak LC RCS is also at the beam center, which suggests that the magnitude of the RCS data is indeed simply tracing out the ALTAIR beam pattern.

[22] Figures 4c and 4d show the 3-D velocity and deceleration of another sample head echo for comparison. Note that this particular head echo's deceleration varies between 5 and 100 km/s^2 over a duration of only 0.1 s. This head echo's peak LC RCS also does not coincide with the center of ALTAIR's beam (peak SNR) and reveals that the parabolic distribution in RCS is due to the time evolution of the meteor as opposed to a radar artifact. This evolution is also attributed to the decreasing meteoroid velocity and increasing atmospheric density and should therefore indicate that the maximum RCS values would occur when the meteoroid releases the maximum amount of kinetic energy. The head echoes with the maximum RCS should therefore occur between 100 and 110 km altitude, where this kinetic energy release is maximized.

[23] Figure 5 contains the results of analysis on 30 VHF head echoes detected at 1820 UT and 2100 UT; none of these head echoes had trails associated with them. Figure 5a shows the 3-D velocity as a function of altitude, where each head echo is indicated by a different symbol. The average 3-D velocity (averaged over the lifetime of a head echo and then over all 20 head echoes) is 69 km/s. The average duration is 0.1 s and the average RCS (LC only) is −27 dBsm. These values are contained in Table 3. Figure 5b shows the deceleration as a function of the radius-density product and indicates that as the radius-density product decreases, the deceleration increases. This result is intuitive: The radii of the meteoroids continue to decrease

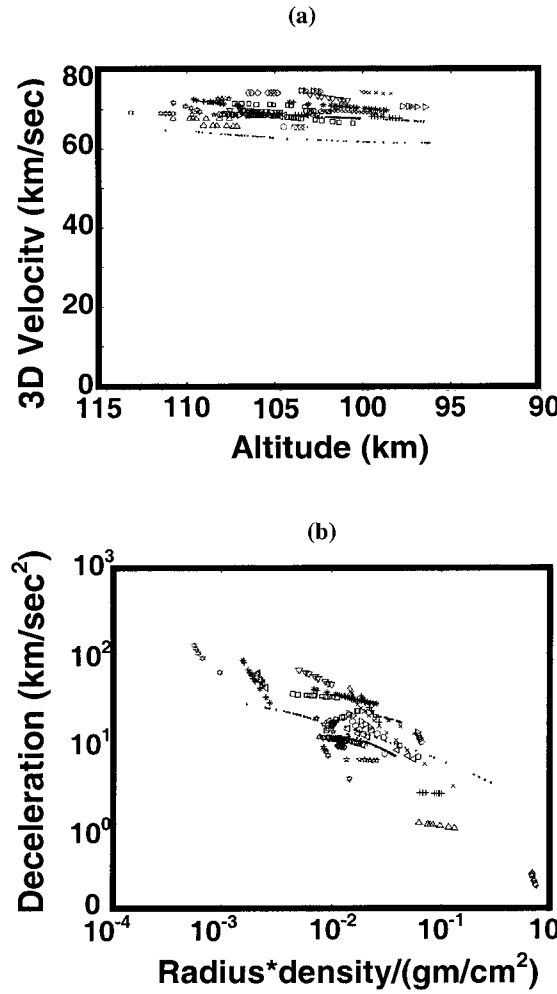

Figure 5. (a) True velocity corrected by monopulse angle data as a function of altitude and (b) associated deceleration as a function of the meteoroid's radius-density product for 30 VHF head echoes.

(assuming a constant density) as they penetrate further into our atmosphere.

5. Summary

[24] ALTAIR detected numerous dual-frequency head echoes during the peak of the Leonid 1998 shower, including 734 VHF echoes (29 min of data) and 472 UHF echoes (17 min of data). Of these, 551 VHF and 328 UHF head echoes were analyzed in order to ascertain altitude, RCS, and range rate characteristics. The monopulse angle data were applied to the head echo range rates in order to determine the 3-D velocities. The 3-D velocity was then used to identify the head echoes as either sporadic or shower and showed that the majority of these head echoes were sporadics. Thirty VHF Leonid head echoes were further analyzed to determine the deceleration dependence on altitude, as well as the radius-density product of the meteoroid particle. Analysis of the Leonid 1999 storm is in progress, and a collection campaign designed to characterize sporadic meteors is also currently planned. The sporadic meteor data will then also be used to calibrate the shower meteor data that were collected during the Perseid and Leonid campaigns.

[25] **Acknowledgments.** The authors acknowledge the contributions of the following people: Ramaswamy Sridharan and Kurt Schwan from the Aeroscape Division at MIT/LL; Tom White, the ALTAIR sensor leader; Scott Coutts and Mark Corbin for valuable input in data collection and analysis; Ken Roth and Chris Moulton from the Ballistic Missile and Defense Technology Division at MIT/LL; Paul Bellaire of AFOSR; Peter Brown of the University of Western Ontario; Marvin Treu. The Leonid 1998 data collection effort, in particular, involved many MIT/LL and Raytheon Range Systems Engineering personnel from the Kwajalein sensors, including Jeff DeLong, Bob Foltz, Tim Mclaughlin, Glen McClellan, Bill Riley, Dave Gibson, Leroy Sievers, Dave Shattuck, Andy Frase, and Wil Pierre-Mike for software and hardware support. The Department of the Army under Air Force contract F19628-/95-C-0002 sponsored this work. Opinions, interpretation, conclusions, and recommendations are those of the authors and are not necessarily endorsed by the U.S. Army.

References

Close, S., S. Hunt, M. Minardi, and F. McKeen, Analysis of Perseid meteor head echo data collected using the Advanced Research Projects Agency Long-Range Tracking and Instrumentation Radar (ALTAIR), *Radio Sci.*, *35*, 1233–1240, 2000.

Evans, J., Radar observations of meteor deceleration, *J. Geophys. Res.*, *71*, 171–188, 1966.

Fitzgerald, R. J., Effects of range-Doppler coupling on chirp radar tracking accuracy, *IEEE Trans. Aerosp. Electron. Syst.*, *AES-10* (4), 528–532, 1974.

Illingworth, J., and J. Kittler, A survey of the Hough transform, *Comput. Vision Graphics Image Process.*, *44*, 87–116, 1988.

Janches, D., J. D. Mathews, D. D. Meisel, and Q.-H. Zhou, Micrometeor observations using the Arecibo 430 MHz radar, *Icarus*, *145*, 53–63, 2000.

Mathews, J. D., D. D. Meisel, K. P. Hunter, V. S. Getman, and Q. Zhou, Very high resolution studies of micrometeors using the Arecibo 430 MHz radar, *Icarus*, *126*, 157–169, 1997.

McKinley, D. W. R., The meteoric head echo, *J. Atmos. Terr. Phys.*, *2*, 65–72, 1955.

Pellinen-Wannberg, A., and G. Wannberg, Meteor observations with the European incoherent scatter UHF radar, *J. Geophys. Res.*, *99*, 11,379–11,390, 1994.

Pellinen-Wannberg, A., A. Westman, G. Wannberg, and K. Kaila, Meteor fluxes and visual magnitudes from EISCAT radar event rates: A comparison with cross-section based magnitude estimates and optical data, *Ann. Geophys.*, *16*, 1475–1485, 1998.

Skolnik, M. I., *Radar Handbook*, McGraw-Hill, New York, 1990.

Zhou, Q.-H., P. Perillat, J. Y. N. Cho, and J. D. Mathews, Simultaneous meteor echo observations by large aperture VHF and UHF radars, *Radio Sci.*, *33*, 1641–1654, 1998.

S. Close, S. M. Hunt, and F. M. McKeen, MIT Lincoln Laboratory, 244 Wood Street, Lexington, MA 02420, USA. (sigrid@ll.mit.edu)

M. J. Minardi, Department of Electrical Engineering, Wright State University, Dayton, OH 45435, USA.